

Optical excitation of polaronic impurities in $\text{La}_2\text{CuO}_{4+y}$

J. P. Falck, A. Levy, M. A. Kastner, and R. J. Birgeneau

Department of Physics, Massachusetts Institute of Technology, Cambridge, Massachusetts 02139

(Received 9 February 1993)

The temperature dependence of the infrared reflectivity of lightly oxygen-doped $\text{La}_2\text{CuO}_{4+y}$ shows that spectral weight is transferred between free-carrier conductivity and a photoionization band of impurity-bound carriers. The large difference between the optical 0.13-eV and thermal 0.035-eV ionization energy indicates that the impurity states are stabilized by a lattice distortion. It is shown that the line shape as well as the temperature dependence is consistent with absorption from a polaronic impurity state.

The introduction of holes into CuO_2 layers causes insulating La_2CuO_4 to become metallic above $\sim 2\%$ of the Cu-ion density.^{1,2} For lower doping levels, $\text{La}_2\text{CuO}_{4+y}$ with excess oxygen behaves like a doped semiconductor with an impurity binding energy of 0.035 eV.³ Both the binding energy and the impurity density necessary to induce the insulator-to-metal transition are a factor of 10 smaller than expected from purely electronic screening of the hole-impurity Coulomb attraction. It has been suggested² that the small values result from additional screening by the optical-phonon modes. Some of these are known to have large dipole moments as seen from the large difference between the static dielectric constant $\epsilon_s \simeq 30$ and the optical frequency value $\epsilon_\infty = 5$. With such a large difference, the charge carriers are expected to form polarons, and evidence that photoexcited electrons and holes do so has been recently reported.⁴ In this paper we show evidence of electron-phonon (EP) coupling in the bound state of the impurity as well.

In doped samples, two midinfrared-absorption bands appear in the optical conductivity spectrum, one centered at ~ 0.5 eV and the other at ~ 0.13 eV.^{5,6} Two bands with similar energies appear in photoinduced absorption data on undoped La_2CuO_4 .⁷ Several models have been proposed to explain these bands. In particular, Thomas *et al.*⁶ have pointed out that the electron-phonon coupling is strong enough to make the optical ionization energy of impurities much larger than the thermal ionization energy. These authors have proposed that the 0.5-eV band results from this optical ionization and that the 0.13-eV band arises from magnetic excitations. Photoinduced absorption measurements, however, indicate that the 0.13-eV band is coupled to the optical phonons.^{7,8} The authors of the latter work have suggested that the 0.13-eV band is caused by self-localized polarons.

In this paper we report measurements of the polarized midinfrared-reflectivity spectrum and its temperature dependence for lightly oxygen-doped $\text{La}_2\text{CuO}_{4+y}$ single crystals. The oscillator strength is found to be transferred from the ~ 0.13 -eV absorption band into the free-carrier conductivity with increasing temperature showing that the 0.13-eV band, rather than the one at ~ 0.5 eV, results from photoionization of holes bound to oxygen acceptors. A model in which the impurity-trapped hole is coupled to the optical-phonon modes pro-

vides a good fit to the data with parameters consistent with other experiments.

Single crystals of La_2CuO_4 were grown by the top-seeded solution growth method using CuO flux.⁹ A crystal was cut with area ~ 5 mm² and thickness ~ 2 mm. The crystal was doped with excess oxygen by annealing in an oxygen-rich atmosphere. This results in a measured Néel temperature of $T_N = 250$ K corresponding to an excess oxygen concentration of $y = 0.014(3)$ as determined by previous measurements.¹⁰ The consequent hole concentration is estimated from Hall data³ to be 0.008 of the Cu ion density. For comparison, we annealed the same crystal in vacuum at 1170 K for 30 min, leaving a reduced La_2CuO_4 crystal with $T_N = 322$ K. A sharp peak at T_N in the magnetic susceptibility indicates that the oxygen is distributed homogeneously for both values of T_N . The annealing process is known to deplete the surface of copper to a depth of roughly 2 μm . Therefore several micrometers were ground off before polishing, and the surfaces were subsequently etched for 20 min in a solution of 1% Br in methanol. The reflectivity was measured on a tetragonal (100) surface, allowing polarization of the light parallel and perpendicular to the CuO_2 layers. The spectrum was measured at $\sim 10^\circ$ incidence in the energy range 0.1–3.1 eV. The reflectivity was normalized to that of an Al mirror, whose absolute reflectivity was measured by removing it and placing the detector in the incident beam. The accuracy of the absolute reflectivity is ~ 0.02 .

The reflectivity spectra are displayed in Fig. 1(a). The out-of-plane spectrum shows no structure except a sharp reduction in the reflectivity for $\hbar\omega \leq 0.19$ eV. This decrease results from optical phonons near 0.08 eV.¹¹ The in-plane reflectivity spectrum for the undoped crystal is almost identical to the out-of-plane spectrum. For the doped crystal, however, the in-plane reflectivity spectrum is enhanced throughout the region from 0.1 to 0.75 eV with a maximum at 0.1 eV. The strength of the 0.1-eV reflectivity peak decreases rapidly as the temperature increases. The midinfrared-absorption processes are clearly connected with the introduction of doping-induced carriers. Furthermore, only the in-plane reflectivity spectrum changes with doping. Thus the midinfrared-absorption processes are confined to the CuO_2 sheets.

The reflectivity data were transformed to give the com-

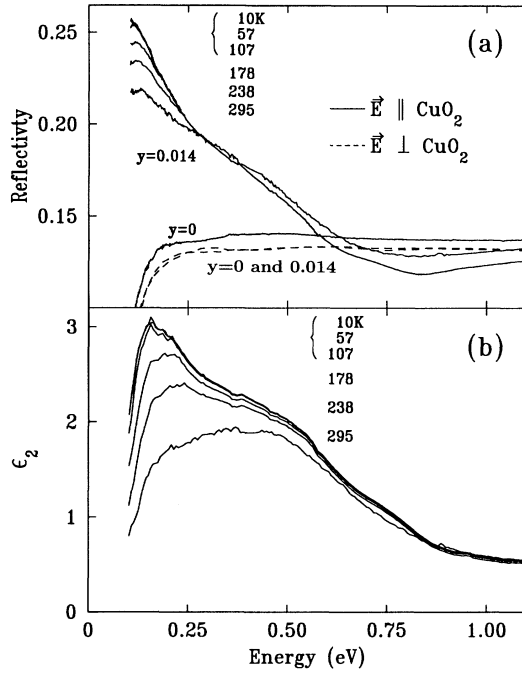


FIG. 1. (a) Reflectivity spectra of $\text{La}_2\text{CuO}_{4+y}$ with $y=0$ and 0.014 . The in-plane spectra for the doped sample are indistinguishable below ~ 100 K. Above 0.3 eV they are only displayed at 10 and 295 K with the latter having the higher reflectivity. (b) In-plane $\epsilon_2(\omega)$ for the oxygen-doped sample.

plex dielectric function using the Kramers-Kronig relations. The results in the 0.1 – 0.2 -eV range are somewhat dependent on the low-energy extrapolation. Because the spectrum is dominated by phonon excitations for $\hbar\omega \leq 0.09$ eV, reflectivity measurements at lower energies would not improve the accuracy of the electronic absorption spectrum. Instead, we used a calculated reflectivity spectrum for a Lorentzian absorption band centered at 0.13 eV. We estimate the uncertainty in ϵ_2 at 0.15 eV to be of order 5% . At high energies ($\hbar\omega > 3.0$ eV), we matched published ultraviolet single-crystal reflectivity data¹¹ to our spectra. Perturbations of the high-energy extrapolation had no measurable impact on the dielectric spectrum below 1.5 eV. In Fig. 1(b) we display the imaginary part of the dielectric constant ϵ_2 . Two separate absorption peaks are clearly distinguished, a broad feature centered at ~ 0.5 eV and a narrower one at ~ 0.13 eV. It is evident that only the 0.13 -eV absorption band is strongly T dependent. In this paper we will only be concerned with the 0.13 -eV band.

The decrease of the oscillator strength in the 0.13 -eV band between 100 and 400 K coincides with an increase of the free-carrier density as evinced by the temperature dependence of the Hall coefficient.³ For a sample with $T_N = 250$ K, the number of free carriers reaches $0.004(1)$ per Cu ion at 300 K. Because of a large contribution from hopping conductivity, it is not possible to determine the binding energy of the impurities accurately for this sample. However, a sample with $T_N = 310$ K has negligible hopping conductivity. For the latter the Hall density increases with T as $\exp[-E_b/k_B T]$ for $40 < T < 300$ K,

giving the binding energy $E_b = 0.035$ eV. By integrating $\int \omega \epsilon_2 d\omega = 2\pi^2 N_{\text{eff}}^* e^2 / m^*$ at 10 and 295 K, we find that the effective number of carriers, N_{eff}^* , involved in the 0.13 -eV absorption decreases by $0.0045(10)$ of the Cu-ion density. To calculate this number, we have used an effective mass of $m^* = 2m_0$. This is the mass consistent with a Coulombic potential model of the bound state² as well as with the value yielding a total oscillator strength of $N_{\text{eff}}^* \approx 1$ when integrated over the entire charge-transfer excitation in undoped La_2CuO_4 .¹¹ Thus the decrease in spectral weight of the 0.13 -eV band is the same as the increase in spectral weight of the dc conductivity. This is strong evidence that the 0.13 -eV band results from photoionization of the impurities. We show below that the detailed T dependence of the reflectivity is consistent with this interpretation.

The optical excitation energy ~ 0.13 eV is almost a factor of 4 larger than the thermal activation energy $E_b = 0.035$ eV measured from the Hall effect. This situation is quite common in ionic insulators in which the charge carrier, bound to the impurity, is strongly coupled to the optical phonons, causing a lattice distortion around the impurity site. During optical ionization of the impurity, the lattice is usually assumed to be frozen, obeying the Frank-Condon (FC) principle. Thus the charge carrier must overcome its polaronic binding energy in addition to the impurity binding energy in order to delocalize. During thermal activation, by contrast, the lattice has time to relax, and so only the impurity binding energy must be overcome.

We know that photoexcited carriers in undoped La_2CuO_4 form large Fröhlich polarons⁴ with an intermediate coupling constant $\alpha_p = 5.7$. The average energy $\hbar\omega_0$ of the phonons involved is experimentally determined to be 0.043 eV.⁴ These polarons are extended and can move freely with a polaronic mass enhancement of order ~ 2 . When the charge carrier is trapped by an impurity, the strength of the EP interaction is expected to be even stronger.¹² In lightly oxygen-doped $\text{La}_2\text{CuO}_{4+y}$ the localization length of the impurity state is measured to be 8 \AA ,² implying that the localized polarons are still large. We therefore assume that the carriers are strongly enough coupled to optical modes for the lattice to be frozen during an optical excitation. Following Ref. 13, we write the total wave function as a product of an electronic and an harmonic part and enforce the FC principle by applying the Condon approximation in which the electronic matrix element is assumed to be independent of the lattice configuration. The imaginary part of the dressed dielectric function can then be written as

$$\epsilon_2(\omega) = \sum_{n=-\infty}^{\infty} W_n \epsilon_2^0(\omega - n\omega_0). \quad (1)$$

Here ϵ_2^0 is the response of the system in the absence of EP coupling and W_n is the probability that the transition occurs with the creation of n phonons. The latter is the thermally averaged overlap of the initial and final lattice configurations given by

$$W_n = \exp[nz - S \coth(z)] I_n[S \operatorname{csch}(z)], \quad (2)$$

where $z = \hbar\omega_0/2k_B T$, $I_n(x)$ is the modified Bessel function, and S is the Huang-Rhys factor. In the strong-coupling limit with $S \gg 1$, the stable lattice configuration in the initial state is strongly displaced relative to the final configuration and only excited final states have a nonvanishing overlap with the initial configuration. In this limit, W_n approaches a Gaussian distribution centered around S with a temperature-dependent standard deviation $\sqrt{S \coth(z)}$. In the opposite limit $S \rightarrow 0$, the phonon coupling vanishes and $W_n \rightarrow \delta_{n,0}$.

Consider now an optical excitation from a localized acceptor state into the valence band. The dielectric function in the absence of EP coupling can generally be expressed as

$$\epsilon_2^0(\omega', T) = \frac{2\pi^2 N_A e^2}{m^* \omega'} \Gamma(\omega') \times \left[\frac{2}{e^{\beta(\mu - E_b)} + 2} - \frac{1}{e^{\beta(\hbar\omega' - E_b + \mu)} + 1} \right], \quad (3)$$

where $\beta = 1/k_B T$, μ is the chemical potential, and $\omega' = \omega - n\omega_0$. The top of the valence band is defined as zero energy. $\Gamma(\omega')/\omega'$ is the ϵ_2 spectrum one would have seen at zero temperature if there were no EP coupling. The temperature dependence is dominated by the carrier occupation in the acceptor band given by the first term in the square brackets. Here the factor of 2 ensures that there is no double occupancy for the localized state. The second term is the occupation of free carriers in the valence band which gives rise to induced emission. We model the change in the position of the Fermi level as a function of temperature by using a simple compensated acceptor-band model. The behavior of the chemical potential is determined by requiring that the total number of localized and free carriers be constant; thus,

$$P_v(T) e^{-\beta\mu} + \frac{2N_A}{e^{\beta(\mu - E_b)} + 2} = N_A - N_D. \quad (4)$$

The first term on the left side represents the total number of holes thermally excited into the valence band at a temperature T . It is determined by adding up all the states in the valence band weighted by their occupation number assuming $k_B T \ll \mu \simeq E_b$. For a two-dimensional (2D) band edge, $P_v(T) = m^* k_B T / \pi L_z \hbar^2$, where L_z is the lattice spacing in the third direction.

The model can best be compared to the data by studying the difference $\epsilon_2(\omega, T) - \epsilon_2(\omega, 238 \text{ K})$ displayed in Fig. 2. The reflectivity data in Fig. 1(a) show a decrease in the strength of the 0.5-eV band between 238 and 295 K. Thus we use the 238-K scan to subtract off the 0.5-eV absorption. The resulting peak at ~ 0.13 eV has a half-width of ~ 0.07 eV. The long high-energy tails may result from a weak temperature dependence of the 0.5-eV band. The dominant response to increasing temperature is a reduction in the overall oscillator strength in the 0.13-eV band with little change in shape as the localized carriers are thermally ionized.

In order to apply Eqs. (1)–(4) to the data, we use $E_b = 0.035$ eV, $\hbar\omega_0 = 0.043$ eV, and $N_A - N_D = 0.008$ per Cu ion. The last number, based on an extrapolation of

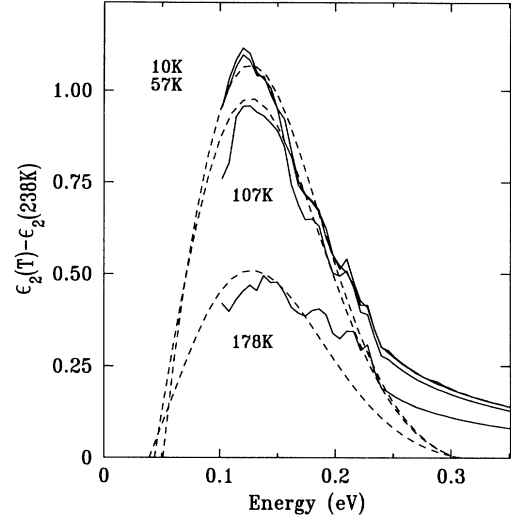


FIG. 2. In-plane difference spectrum $\epsilon_2(\omega, T) - \epsilon_2(\omega, 238 \text{ K})$ for different temperatures. The dashed lines represent best fits to the data using the model and parameters discussed in the text.

the Hall density data³ to infinite temperature, is only known to a factor of 2. This uncertainty has no impact upon our analysis since the T dependence of ϵ_2 is only weakly dependent upon $N_A - N_D$. The compensation ratio N_D/N_A is determined from a fit to the T dependence of the reflectivity as discussed below.

The peak position, the linewidth, and the line shape are all properties determined solely by S . Indeed, the peak energy to first order is simply $E_b + S\hbar\omega_0$; for $\hbar\omega_0 = 0.043$ eV and $E_b = 0.035$ eV this gives $S \sim 2.2$. Generally for $S > 1$ the shift of the peak position and the broadening are weakly dependent on the detailed form of $\Gamma(\omega')$. For convenience, we use $\Gamma(\omega')$ calculated for ionization of a hole bound in a Coulombic impurity potential.¹⁴ The best fit, displayed in Fig. 2, gives $S = 2.4$. The fit clearly recreates the position of the center frequency and the overall width as well as the general temperature dependence. To test the sensitivity to the choice of $\Gamma(\omega')$, we also tried a narrow electronic cross section $\Gamma(\omega') = \delta(\hbar\omega' - E_b)$. The best fit for the latter yields $S = 2.7$ with a line shape indistinguishable from the Coulombic fit. Thus, independent of the details, we find $S = 2.5 \pm 0.2$.

To study the temperature dependence in more detail, we compare in Fig. 3 the in-plane reflectivity at 0.11 eV as a function of temperature with that calculated from our model. The reflectivity is temperature independent below ~ 100 K, reflecting the negligible fraction of carriers thermally excited from the localized states. At higher temperatures this fraction increases, decreasing the strength of the 0.13-eV band. The real part of the dielectric response $\epsilon_1(\omega)$ is extracted from the calculated $\epsilon_2(\omega)$ using the Kramers-Kronig relations. The reflectivity is then calculated from the total complex dielectric response $\epsilon(\omega) = \epsilon_0 + \epsilon_1(\omega) + i\epsilon_2(\omega)$. Using $\Gamma(\omega')$ from the Coulombic model, with $S = 2.4$, we vary

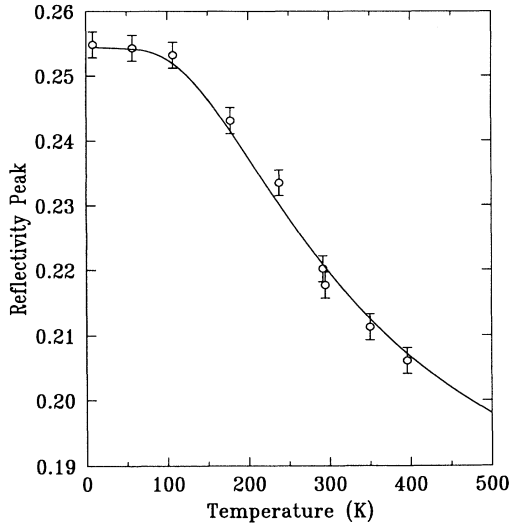


FIG. 3. Temperature dependence of the in-plane reflectivity at 0.11 eV. The solid line represents the best fit to the data using the model and parameters discussed in the text.

the compensation ratio N_D/N_A and the effective dielectric constant $\bar{\epsilon}_0$. The fit, displayed as a solid line in Fig. 3, gives $\bar{\epsilon}_0=5.7$ and $N_D/N_A=0.5$. The activated T dependences in Eqs. (3) and (4) make the fit insensitive to N_A-N_D and N_D/N_A as long as N_D is not much smaller than N_A . Good fits are found for $N_D/N_A=0.5\pm 0.1$ for a reasonable range of N_A-N_D .

The optimized effective dielectric constant $\bar{\epsilon}_0=5.7$ should be compared with the high-frequency dielectric constant in the undoped sample, $\epsilon_\infty=4.8$. The slight difference probably results from a small contribution to the dielectric constant at low energies from the 0.5-eV absorption band in the doped sample.

We have no independent measure of the compensation ratio. However, from transport measurements we know that the Fermi level is pinned in the impurity band over the entire temperature range of activated conductivity. Applying Eq. (4), this requires the compensation ratio to

be larger than 0.3, consistent with our value 0.5 ± 0.1 .

The Huang-Rhys factor $S=2.5$ is the average number of phonons created in the ionization process, whereas $\alpha_p=5.7$ is the number of phonons involved in the large polaron. We do not therefore consider the difference between α_p and S to be surprising.

The midinfrared absorption is a common feature of the cuprates. In $\text{La}_2\text{CuO}_{4+y}$ and $\text{Nd}_2\text{CuO}_{4-y}$ as well as $\text{YBa}_2\text{Cu}_3\text{O}_{6+y}$, two infrared-absorption peaks become stronger with doping,⁶ one in the energy range 0.5–0.75 eV and the other in the range 0.13–0.16 eV. It would be quite remarkable if the origin of these absorption processes were fundamentally different for the different materials. Thus we expect our results to be a general feature of high- T_c cuprates. In $\text{Nd}_2\text{CuO}_{4-y}$ the low-energy absorption centered at 0.16 eV has been found to broaden with increasing temperature in a linear fashion,⁶ but no decrease in oscillator strength has been observed up to 300 K. This behavior can easily be explained within the framework of our results if the binding energy of the donor impurity in the sample studied is ≥ 0.09 eV. By contrast, a reduction of photoinduced absorption in the range 0.13–0.16 eV occurs⁷ near ~ 20 K in both Nd_2CuO_4 and La_2CuO_4 , suggesting a much lower binding energy for photocarriers.

In summary, we have shown that the 0.13-eV absorption process in $\text{La}_2\text{CuO}_{4+y}$ is due to photoexcitation of localized holes from impurities. The excitation spectrum can be understood by assuming that the hole is coupled with intermediate strength to optical-phonon modes. It is not surprising that carriers bound to impurities form polarons since we showed earlier that photoexcited carriers do so. Related behavior in other systems suggests that polaronic impurity states are a generic feature of the high- T_c cuprates. Finally, we note that recent work by Perkins *et al.*¹⁵ suggests that the 0.5-eV peak results from exciton-multimagnon absorptoin processes.

We would like to thank D. Emin, A. Millis, P. A. Lee, and P. M. Platzman for invaluable discussions. This work was supported by the National Science Foundation Grant Nos. DMR 90-22933 and DMR 90-14839.

¹N. W. Preyer *et al.*, Phys. Rev. B **44**, 407 (1991).

²C. Y. Chen *et al.*, Phys. Rev. B **43**, 392 (1991).

³N. W. Preyer *et al.*, Phys. Rev. B **39**, 11 563 (1989).

⁴J. P. Falck *et al.*, Phys. Rev. Lett. **69**, 1109 (1992).

⁵For a recent review, see D. B. Tanner and T. Timusk, in *Physical Properties of High Temperature Superconductors III*, edited by D. Ginsberg (World Scientific, Singapore, 1992).

⁶G. A. Thomas *et al.*, Phys. Rev. B **45**, 2474 (1992); G. A. Thomas *et al.*, Phys. Rev. Lett. **67**, 2906 (1991).

⁷Y. H. Kim *et al.*, Phys. Rev. Lett. **67**, 2227 (1991); Y. H. Kim *et al.*, Phys. Rev. B **36**, 7252 (1987).

⁸C. M. Foster *et al.*, Solid State Commun. **71**, 945 (1989).

⁹P. J. Picone *et al.*, J. Cryst. Growth **85**, 576 (1987).

¹⁰D. C. Johnston *et al.*, Physica C **153-155**, 572 (1988).

¹¹S. Uchida *et al.*, Phys. Rev. B **43**, 7942 (1991).

¹²D. Emin and T. Holstein, Phys. Rev. Lett. **36**, 323 (1976).

¹³J. Bourgoin and M. Lannoo, *Point Defects in Semiconductors* (Springer, New York, 1983).

¹⁴H. Bethe, *Handbuch der Physik* (Julius Springer, Berlin, 1933), Vol. 24/1, Ziff 47.

¹⁵J. D. Perkins *et al.* (unpublished).